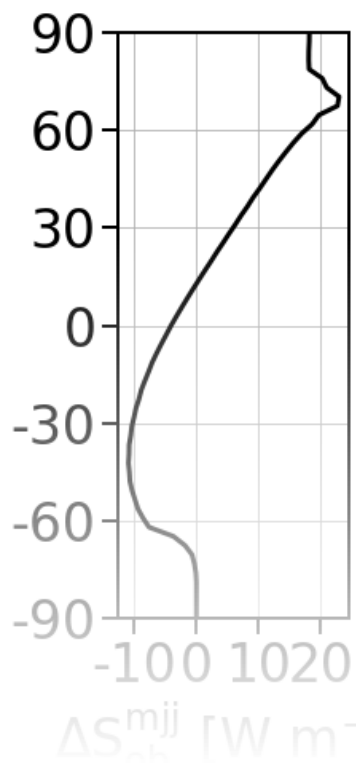

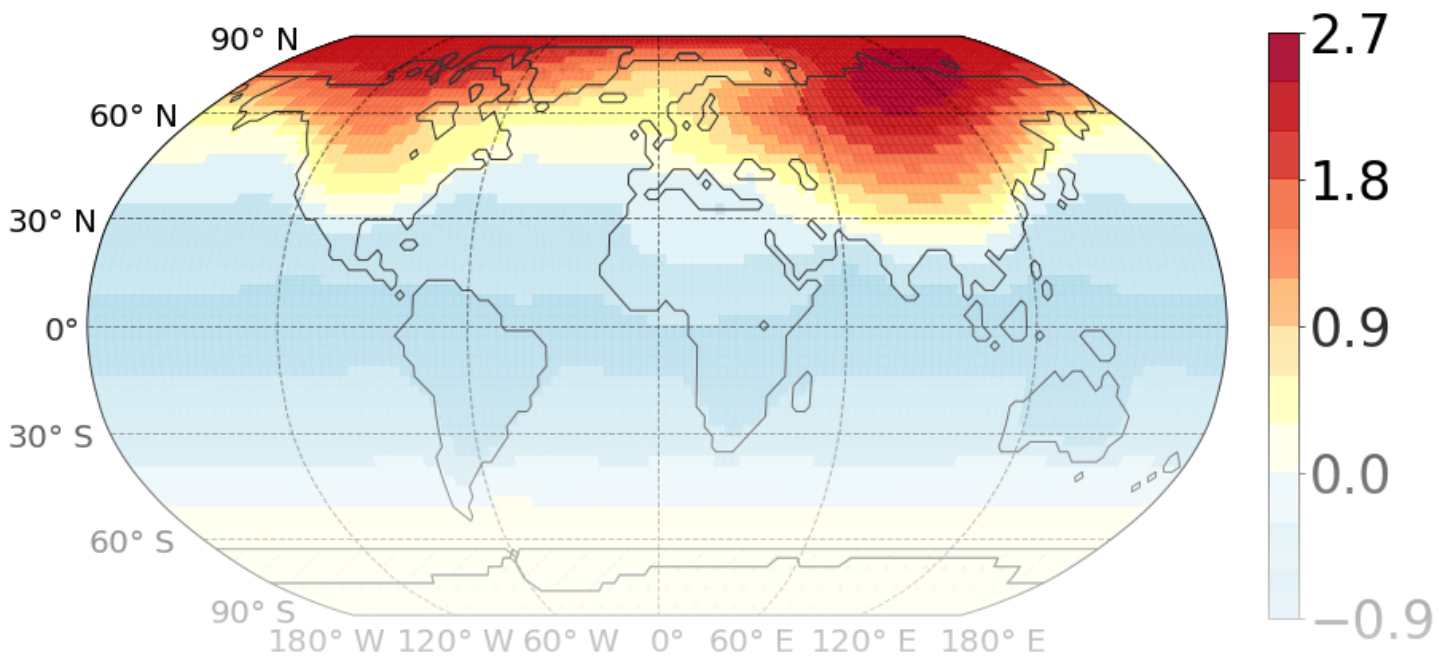

Simulation of climate variability since the Last Glacial using climate models of varying complexity

---

▶ *Elisa Ziegler*, ▶ *Kira Rehfeld*

CL1.9 Orbital forcing, tectonics, and global climate change

uni-heidelberg.de/palaeoclimate-dynamics

Examination of the extremes in orbital forcing with an energy balance model (TransEBM)

Experiment

- set one orbital parameter to a natural extreme
- keep all other forcings constant
- here with TransEBM, but repeat with models of different complexity

Examine how orbital forcings

- drive climatic changes
- interact with other components of the climate system

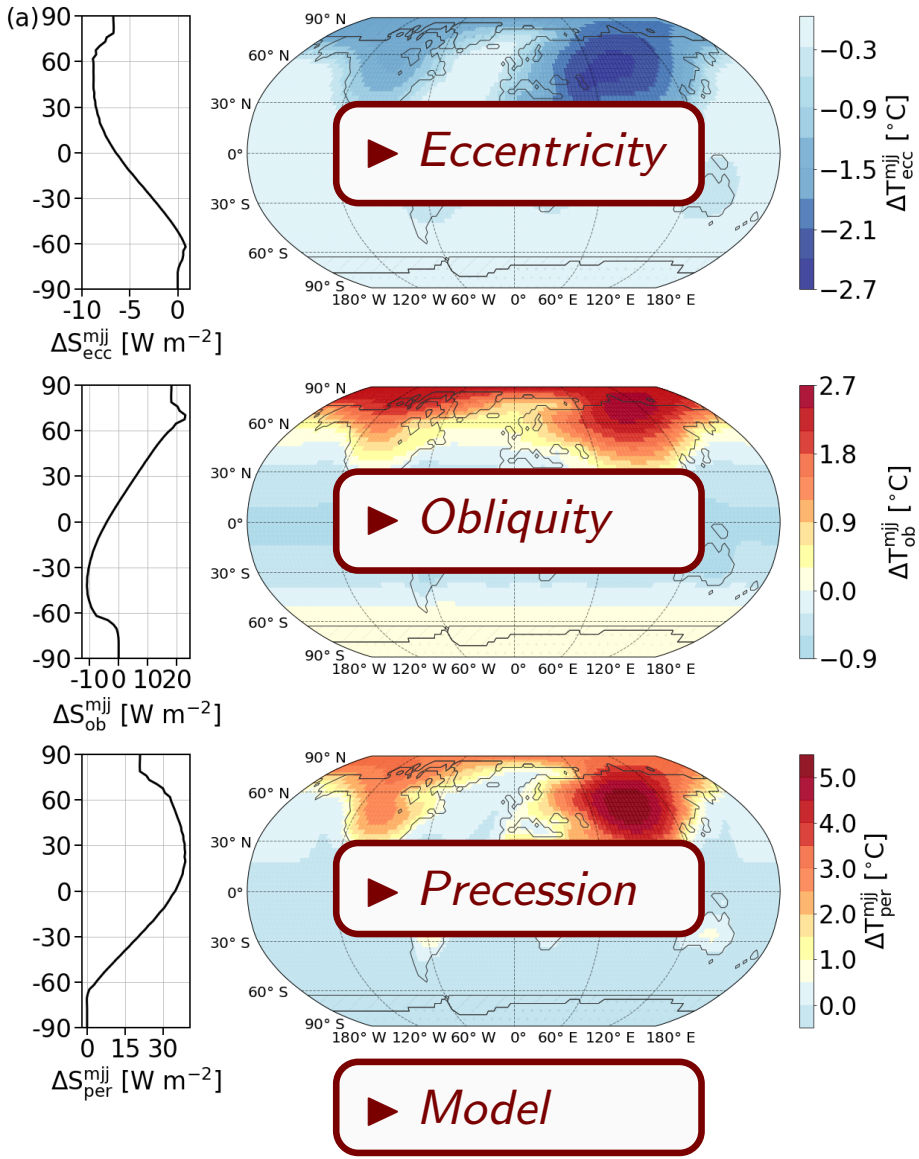

Eccentricity: May-Jun-Jul

Solar insolation and temperature difference between eccentricity = 0.06 and 0.005

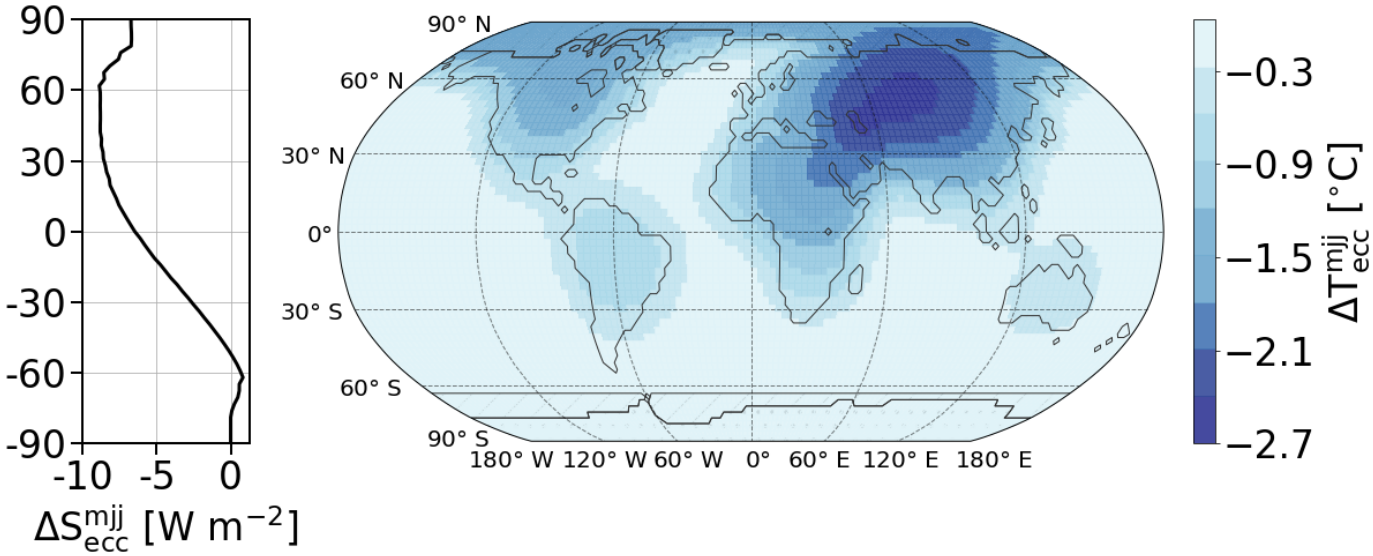

- ▶ *Nov – Dec – Jan*
- ▶ *Annual*
- ▶ *Obliquity*
- ▶ *Precession*
- ▶ *Model*

Experiment setup:

- perihelion at vernal equinox
- obliquity = 0.398808
- S_0 = 1362 W/m^2, CO_2 = 315 ppm
- 1950 land-sea mask [Zhuang et al., 2017]

Results:

- decreased summer insolation in northern hemisphere with larger eccentricity
- largest effect in middle latitudes

Eccentricity: Nov-Dec-Jan

Solar insolation and temperature difference between eccentricity = 0.06 and 0.005

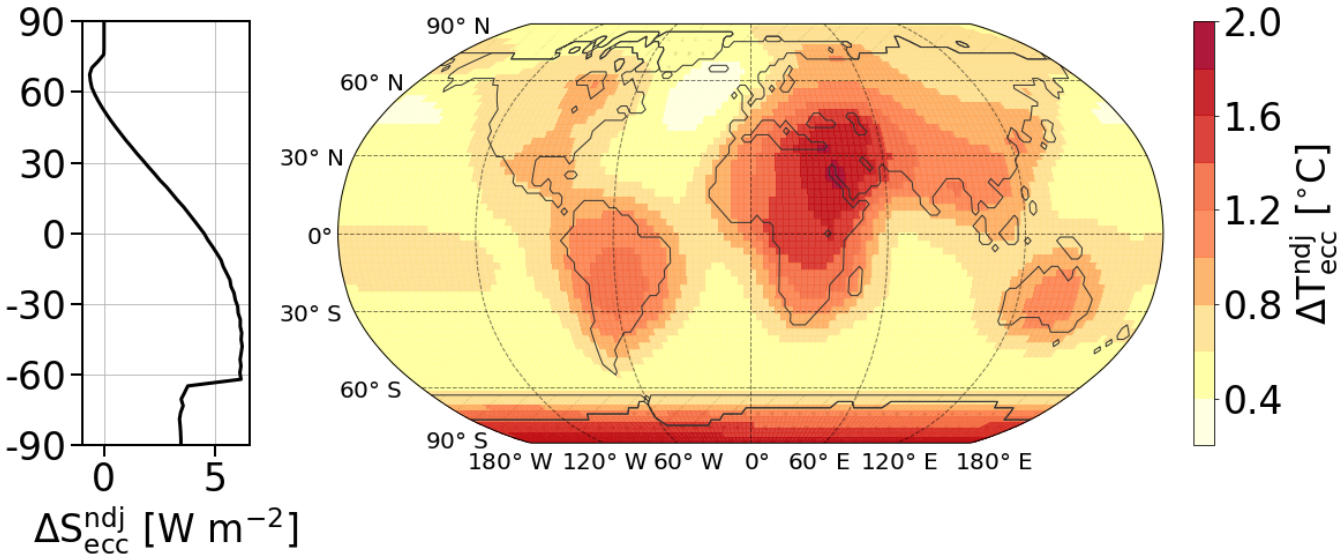

- ▶ *May – Jun – Jul*
- ▶ *Annual*
- ▶ *Obliquity*
- ▶ *Precession*
- ▶ *Model*

Experiment setup:

- perihelion at vernal equinox
- obliquity = 0.398808
- S_0 = 1362 W/m^2, CO_2 = 315 ppm
- 1950 land-sea mask [Zhuang et al., 2017]

Results:

- increased summer insolation in southern hemisphere with larger eccentricity
- largest effect in middle latitudes

Eccentricity: Annual average

Solar insolation and temperature difference between eccentricity = 0.06 and 0.005

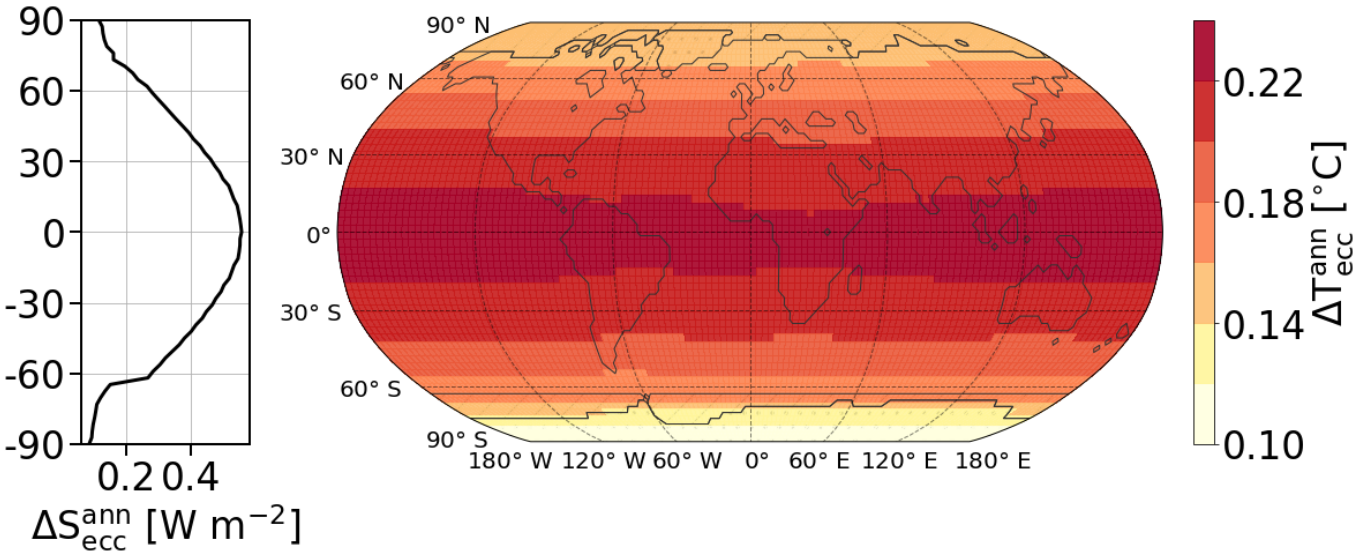

- ▶ *May – Jun – Jul*
- ▶ *Nov – Dec – Jan*
- ▶ *Obliquity*
- ▶ *Precession*
- ▶ *Model*

Experiment setup:

- perihelion at vernal equinox
- obliquity = 0.398808
- S_0 = 1362 W/m^2, CO_2 = 315 ppm
- 1950 land-sea mask [Zhuang et al., 2017]

Results:

- symmetric pattern in both hemispheres
- largest effect in lower latitudes, smaller towards high latitudes

Obliquity: May-Jun-Jul

Solar insolation and temperature difference between

obliquity = 24.5° and 22.1°

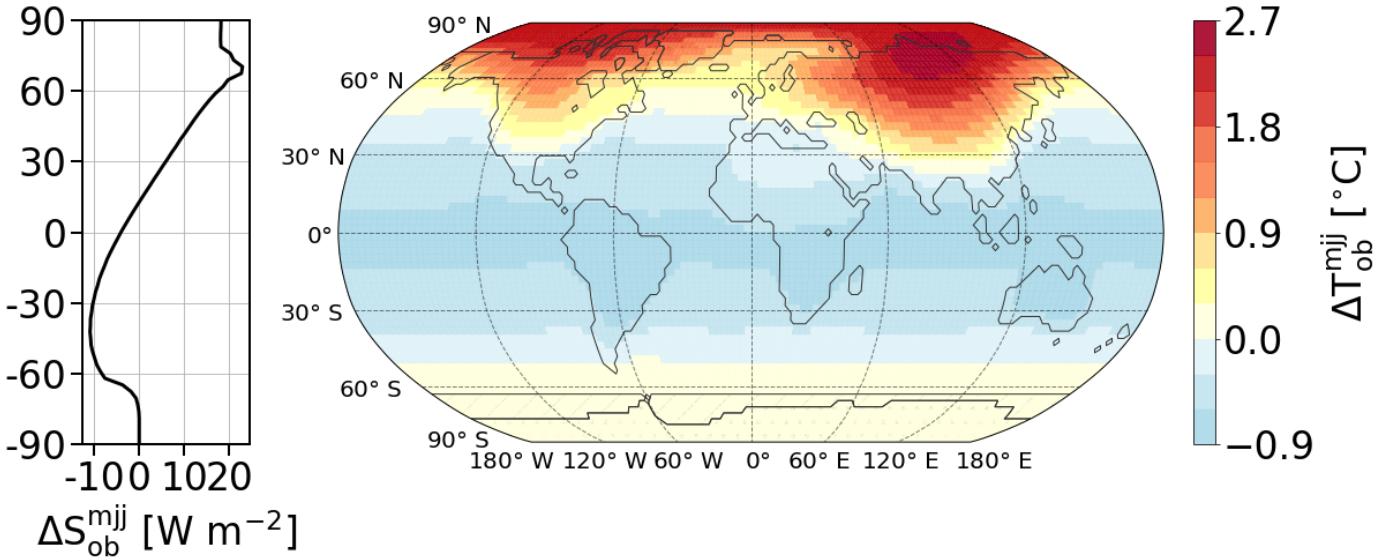

- ▶ *Eccentricity*
- ▶ *Nov – Dec – Jan*
- ▶ *Annual*
- ▶ *Precession*
- ▶ *Model*

Experiment setup:

- perihelion at vernal equinox
- eccentricity 0.0325
- $S_0 = 1362$ W/m^2, $CO_2 = 315$ ppm
- 1950 land-sea mask [Zhuang et al., 2017]

Results:

- increased insolation in northern, decreased in southern hemisphere with larger obliquity
- largest temperature increase over land in middle latitudes and in high latitudes

Obliquity: Nov-Dec-Jan

Solar insolation and temperature difference between obliquity = 24.5° and 22.1°

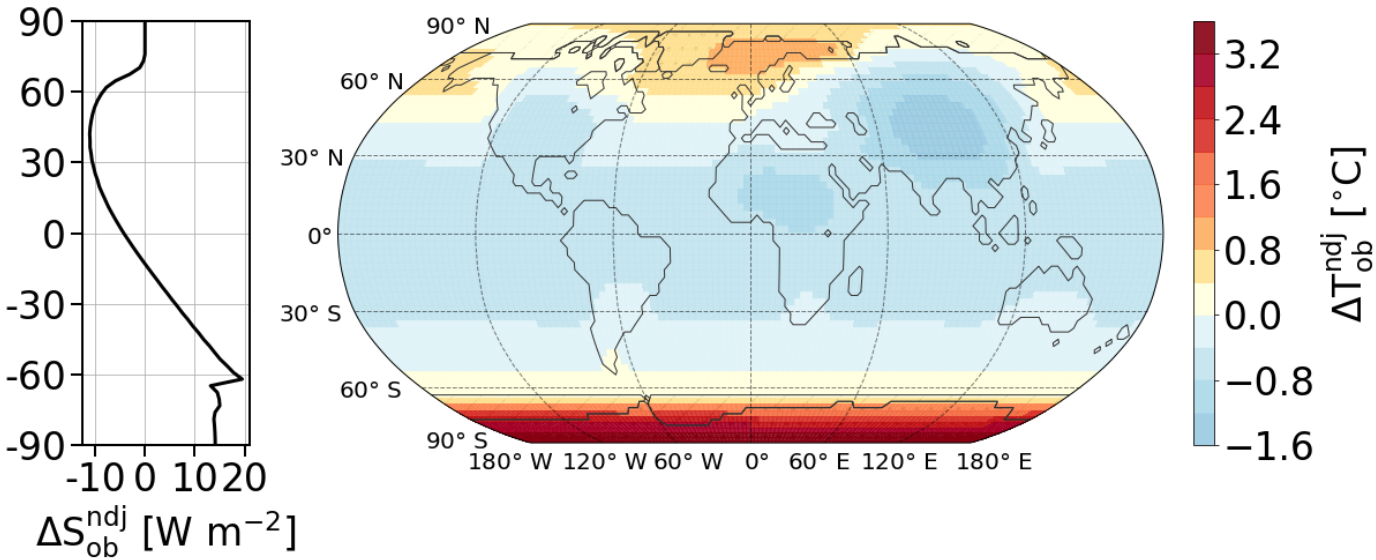

- ▶ *Eccentricity*
- ▶ *May – Jun – Jul*
- ▶ *Annual*
- ▶ *Precession*
- ▶ *Model*

Experiment setup:

- perihelion at vernal equinox
- eccentricity 0.0325
- $S_0 = 1362$ W/m^2, $CO_2 = 315$ ppm
- 1950 land-sea mask [Zhuang et al., 2017]

Results:

- decreased insolation in northern, increased insolation in southern hemisphere with larger obliquity
- largest effect in middle latitudes and over Antarctica

Obliquity: Annual average

Solar insolation and temperature difference between

obliquity = 24.5° and 22.1°

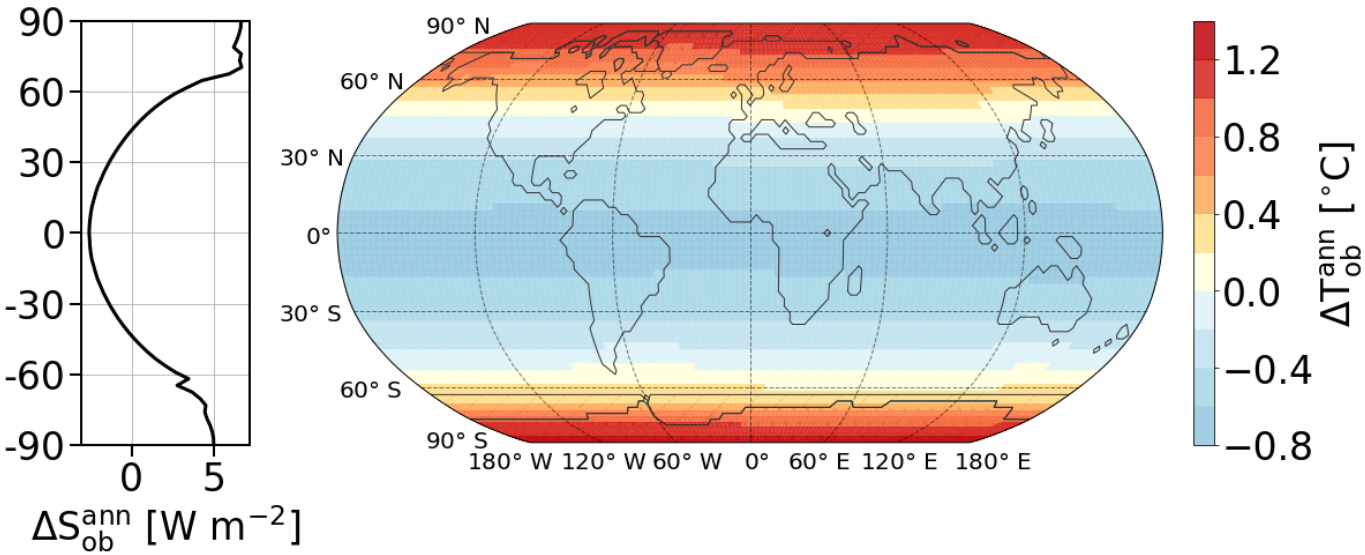

- ▶ *Eccentricity*
- ▶ *May – Jun – Jul*
- ▶ *Nov – Dec – Jan*
- ▶ *Precession*
- ▶ *Model*

Experiment setup:

- perihelion at vernal equinox
- eccentricity 0.0325
- S_0 = 1362 W/m^2, CO_2 = 315 ppm
- 1950 land-sea mask [Zhuang et al., 2017]

Results:

- symmetric pattern
- negative S, T in low latitudes
- increasing S, T towards higher latitudes

Precession: May-Jun-Jul

Solar insolation and temperature difference between perihelion at June vs December solstice

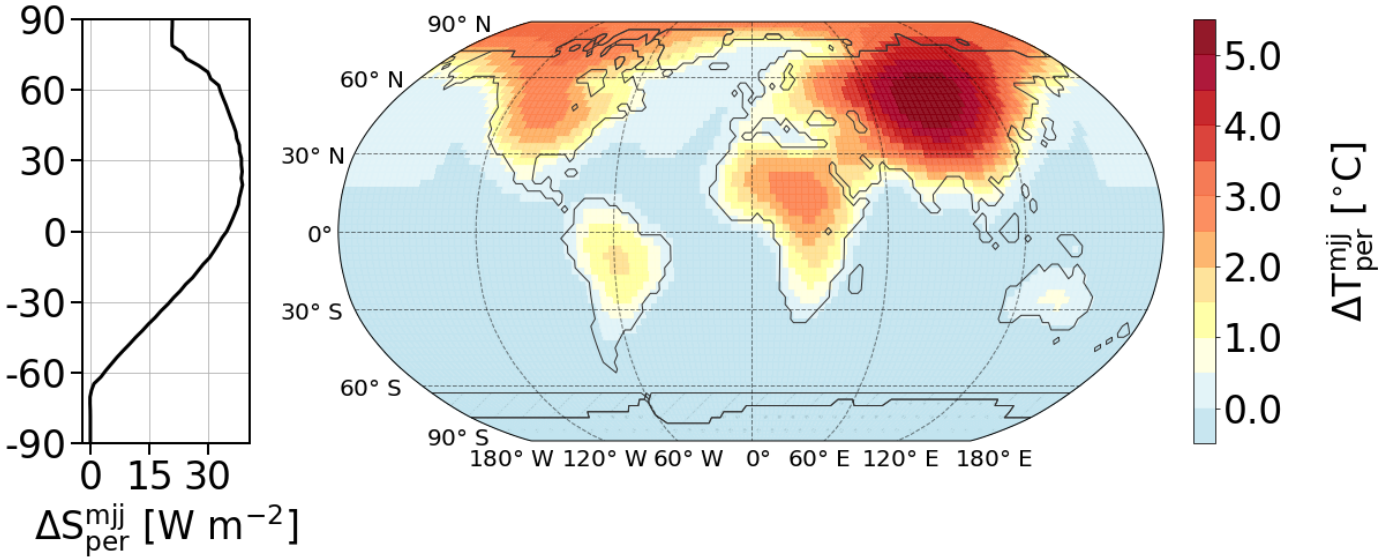

- ▶ *Eccentricity*
- ▶ *Obliquity*
- ▶ *Nov – Dec – Jan*
- ▶ *Annual*
- ▶ *Model*

Experiment setup:

- eccentricity 0.0325
- obliquity = 0.398808
- S_0 = 1362 W/m^2, CO_2 = 315 ppm
- 1950 land-sea mask [Zhuang et al., 2017]

Results:

- increased insolation, especially, in low and middle northern latitudes
- largest temperature increase over Asia

Precession: Nov-Dec-Jan

Solar insolation and temperature difference between perihelion at June vs December solstice

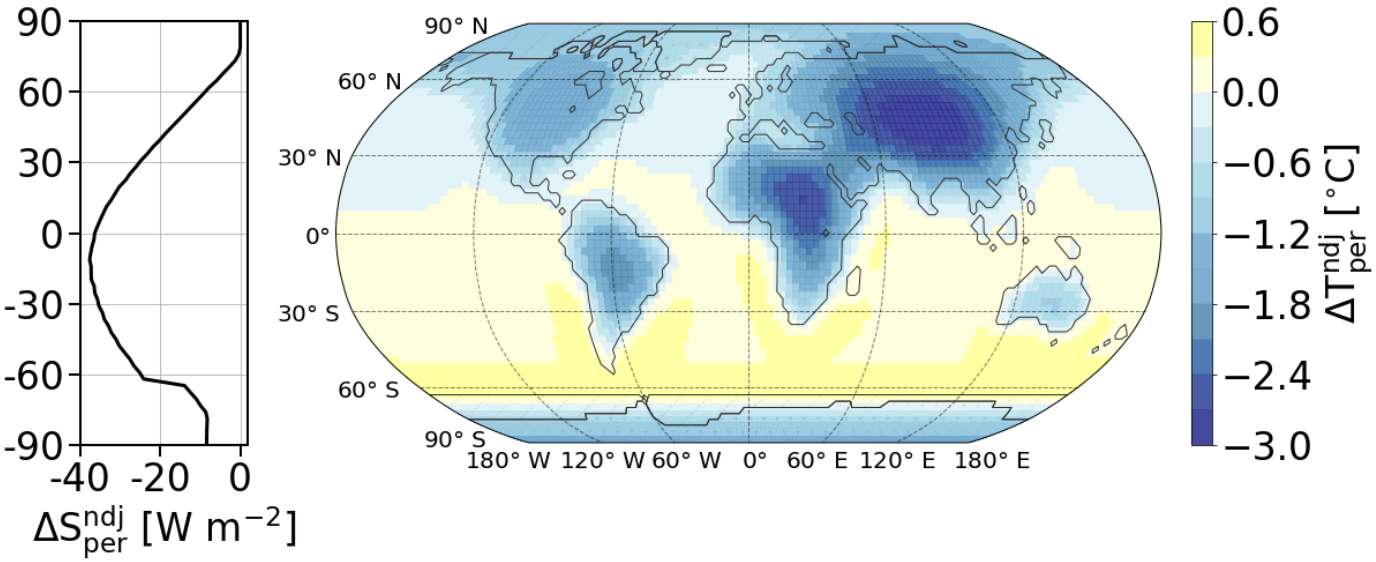

- ▶ *Eccentricity*
- ▶ *Obliquity*
- ▶ *May – Jun – Jul*
- ▶ *Annual*
- ▶ *Model*

Experiment setup:

- eccentricity 0.0325
- obliquity = 0.398808
- S_0 = 1362 W/m^2, CO_2 = 315 ppm
- 1950 land-sea mask [Zhuang et al., 2017]

Results:

- decreased insolation with perihelion at June solstice, especially in lower latitudes
- general decrease in temperatures, largest temperature decrease over Asia and Africa

Precession: Annual average

Solar insolation and temperature difference between perihelion at June vs December solstice

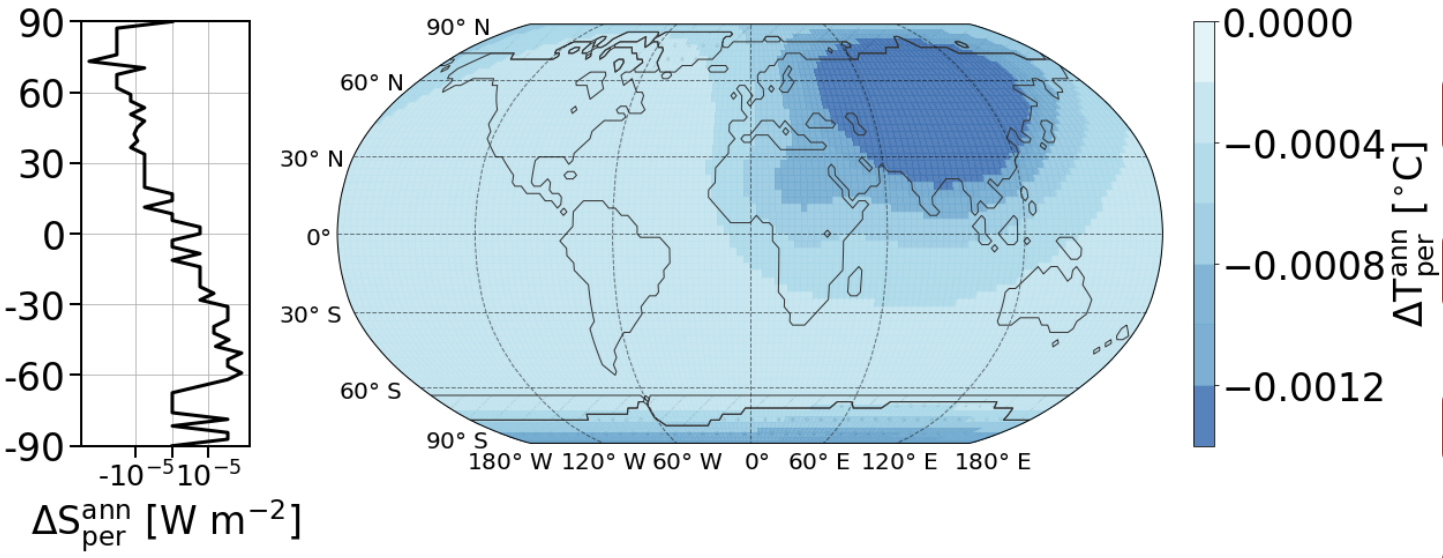

- ▶ *Eccentricity*
- ▶ *Obliquity*
- ▶ *May – Jun – Jul*
- ▶ *Nov – Dec – Jan*
- ▶ *Model*

Experiment setup:

- eccentricity 0.0325
- obliquity = 0.398808
- S_0 = 1362 W/m^2, CO_2 = 315 ppm
- 1950 land-sea mask [Zhuang et al., 2017]

Results:

- virtually now influence on annual average

TransEBM – model specs

Based on model by
[North et al., 1980],
[North et al., 1983],
[Hyde et al., 1989]
[Zhuang et al., 2017], ...

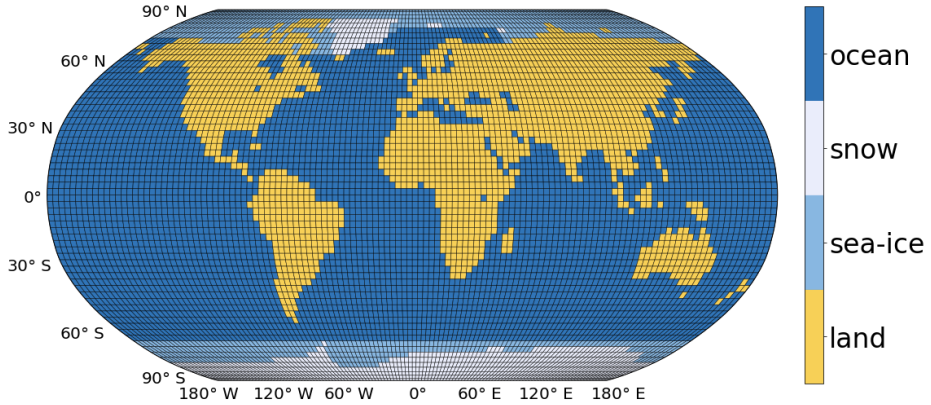

Model extension

- transient
- restarts
- configuration files
- ...

▶ *Start* ▶ *Eccentricity* ▶ *Obliquity* ▶ *Precession*

TransEBM – model specs

grid:	128 x 64 points (2.8° x 2.8°)
input:	CO_2, S_0, orbital configuration, land-sea mask
output:	surface temperature field (+ insolation, heat capacities)
time steps:	48 per year
benchmark:	57,600 yrs/day

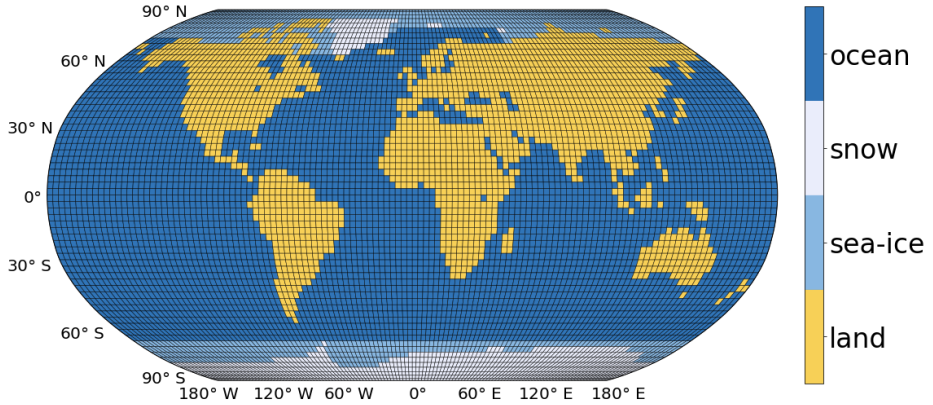

▶ *Start* ▶ *Eccentricity* ▶ *Obliquity* ▶ *Precession*

TransEBM – core equation

elliptical partial differential equation:

$$C(\hat{\mathbf{r}})\frac{\partial T}{\partial t} + A + B \cdot T = \nabla \cdot (D(\hat{\mathbf{r}})\nabla T) + S_0 \cdot S(\hat{\mathbf{r}}, t)a(\hat{\mathbf{r}})$$

solved with full multigrid method
by [Zhuang et al., 2017],
based on [Huang and Bowman, 1992]

▶ *Start* ▶ *Eccentricity* ▶ *Obliquity* ▶ *Precession*

TransEBM – core equation

elliptical partial differential equation:

$$C(\hat{\mathbf{r}})\frac{\partial T}{\partial t} + A + B \cdot T = \nabla \cdot (D(\hat{\mathbf{r}})\nabla T) + S_0 \cdot S(\hat{\mathbf{r}}, t)a(\hat{\mathbf{r}})$$

C: effective heat capacity $[10^6 \mathrm{J/K/m^2}]$
set according to geography

land	ocean	sea ice	snow	atmosphere
1.87	394.47	4.83	1.52	0.79

▶ *Start* ▶ *Eccentricity* ▶ *Obliquity* ▶ *Precession*

TransEBM – core equation

elliptical partial differential equation:

$$C(\hat{\mathbf{r}})\frac{\partial T}{\partial t} + A + B \cdot T = \nabla \cdot (D(\hat{\mathbf{r}})\nabla T) + S_0 \cdot S(\hat{\mathbf{r}}, t)a(\hat{\mathbf{r}})$$

A: outgoing radiation, from satellite data

$A = (210.2 - 5.35 \cdot \log(CO_2/315\text{ppm}))\ \text{W/m}^2$

▶ *Start* ▶ *Eccentricity* ▶ *Obliquity* ▶ *Precession*

TransEBM – core equation

elliptical partial differential equation:

$$C(\hat{\mathbf{r}})\frac{\partial T}{\partial t} + A + B \cdot T = \nabla \cdot (D(\hat{\mathbf{r}})\nabla T) + S_0 \cdot S(\hat{\mathbf{r}}, t)a(\hat{\mathbf{r}})$$

B: outgoing radiation, from satellite data

$B = 2.13 W/m^2/^\circ C$

determines sensitivity of seasonal cycle & feedbacks (water vapor, lapse rate, cloud cover)

▶ *Start* ▶ *Eccentricity* ▶ *Obliquity* ▶ *Precession*

TransEBM – core equation

elliptical partial differential equation:

$$C(\hat{\mathbf{r}})\frac{\partial T}{\partial t} + A + B \cdot T = \nabla \cdot (D(\hat{\mathbf{r}})\nabla T) + S_0 \cdot S(\hat{\mathbf{r}}, t)a(\hat{\mathbf{r}})$$

D: diffusion coefficient

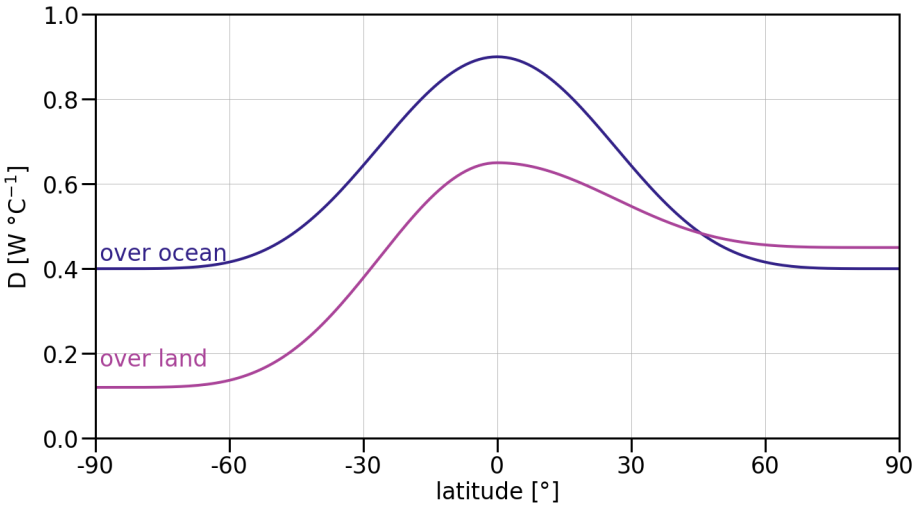

▶ Start ▶ Eccentricity ▶ Obliquity ▶ Precession

TransEBM – core equation

elliptical partial differential equation:

$$C(\hat{\mathbf{r}})\frac{\partial T}{\partial t} + A + B \cdot T = \nabla \cdot (D(\hat{\mathbf{r}})\nabla T) + S_0 \cdot S(\hat{\mathbf{r}}, t)a(\hat{\mathbf{r}})$$

S_0: solar constant

S: insolation distribution
depends on orbital parameters

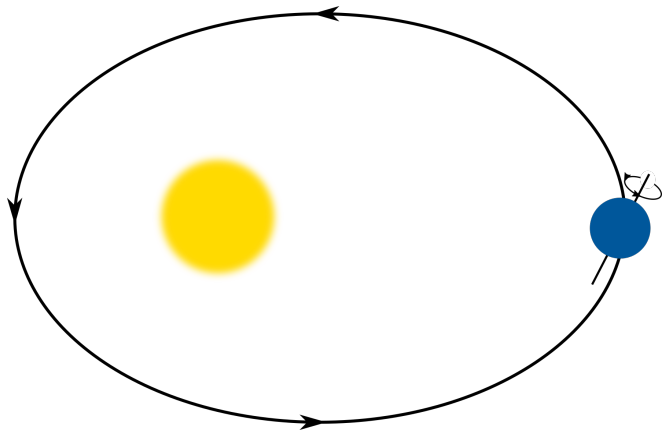

▶ *Start* ▶ *Eccentricity* ▶ *Obliquity* ▶ *Precession*

TransEBM – core equation

elliptical partial differential equation:

$$C(\hat{\mathbf{r}})\frac{\partial T}{\partial t} + A + B \cdot T = \nabla \cdot (D(\hat{\mathbf{r}})\nabla T) + S_0 \cdot S(\hat{\mathbf{r}}, t)a(\hat{\mathbf{r}})$$

a: albedo

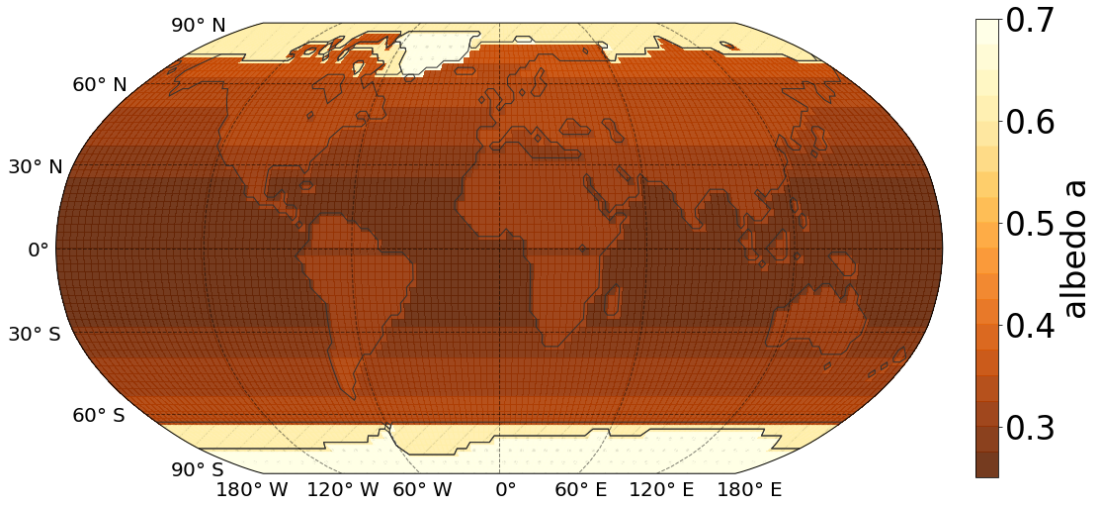

▶ Start ▶ Eccentricity ▶ Obliquity ▶ Precession

20th century model-data comparison

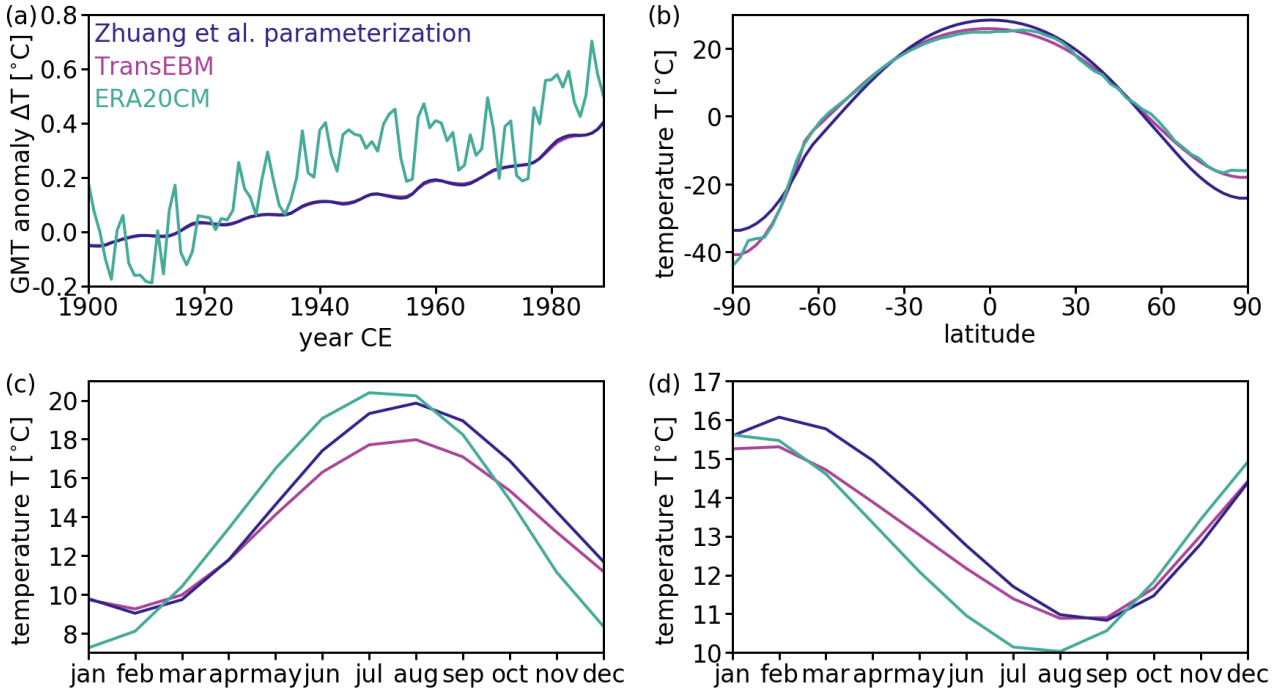

Comparison of a simulation of the twentieth century by TransEBM with the parameterization by [Zhuang et al., 2017] and ERA20CM reanalysis data Hersbach2015. Simulation forced by CO_2 from [Köhler et al., 2017], orbital parameters from [Laskar et al., 2004], solar constant from [Coddington et al., 2016].
(a) Timeseries of the annual temperature anomaly w.r.t. 1900-1929 climatological means. The different parameterizations show little difference and capture the overall trend. The reanalysis shows stronger inter-annual variation.
(b) Average latitudinal profiles. TransEBM agrees with reanalysis data better – esp. in polar regions and around the equator.
(c) and (d) Seasonal temperature profiles in the northern and southern hemisphere. The simulated profiles are both shifted in comparison to the reanalysis. Agreement is better in the southern hemisphere, TransEBM underestimates the seasonal cycle in the northern hemisphere.

▶ *Start* ▶ *Eccentricity* ▶ *Obliquity* ▶ *Precession*

Bibliography i

Coddington, O., Lean, J. L., Pilewskie, P., Snow, M., and Lindholm, D. (2016).
A solar irradiance climate data record.
Bulletin of the American Meteorological Society, 97(7):1265–1282.

Huang, J. and Bowman, K. P. (1992).
The small ice cap instability in seasonal energy balance models.
Climate Dynamics, 7(4):205–215.

Hyde, W. T., Crowley, T. J., Kim, K.-Y., and North, G. R. (1989).
Comparison of GCM and energy balance model simulations of seasonal temperature changes over the last 18,000 years.
Journal of Climate, 2:864–887.

Köhler, P., Nehrbass-Ahles, C., Schmitt, J., Stocker, T. F., and Fischer, H. (2017).
A 156 kyr smoothed history of the atmospheric greenhouse gases CO2, CH4, and N2O and their radiative forcing.
Earth System Science Data, 9(1):363–387.

Laskar, J., Robutel, P., Joutel, F., Gastineau, M., Correia, A. C. M., and Levrard, B. (2004).
A long-term numerical solution for the insolation quantities of the Earth.
Astronomy & Astrophysics, 428(1):261–285.

North, G. R., Cahalan, R. F., and Coakley, J. A. (1980).
Energy-Balance Climate Models.
Rev. Geophys. Space Phys, 16(4):2000–2001.

Bibliography ii

North, G. R., Mengel, J. G., and Short, D. A. (1983).
Simple energy balance model resolving the seasons and the continents: application to the astronomical theory of the ice ages.
Journal of Geophysical Research, 88(C11):6576–6586.

Zhuang, K., North, G. R., and Stevens, M. J. (2017).
A NetCDF version of the two-dimensional energy balance model based on the full multigrid algorithm.
SoftwareX, 6:198–202.